EPJ Photovoltaics **7**, 70303 (2016)
www.epj-pv.org
DOI: 10.1051/epjpv/2016001

Solution-processed In_2S_3 buffer layer for chalcopyrite thin film solar cells

Lan Wang[1,a], Xianzhong Lin[1], Ahmed Ennaoui[2], Christian Wolf[1], Martha Ch. Lux-Steiner[1,3], and Reiner Klenk[1]

[1] Helmholtz-Zentrum Berlin für Materialien und Energie, Hahn-Meitner-Platz 1, 14109 Berlin, Germany
[2] Qatar Environment and Energy Research Institute and Hamad Bin Khalifa University, Education City, Doha, Qatar
[3] Freie Universität Berlin, Fachbereich Physik, Arnimallee 14, 14195 Berlin, Germany

Received: 4 December 2015 / Received in final form: 22 January 2016/ Accepted: 27 January 2016
Published online: 26 February 2016

Abstract We report a route to deposit In_2S_3 thin films from air-stable, low-cost molecular precursor inks for Cd-free buffer layers in chalcopyrite-based thin film solar cells. Different precursor compositions and processing conditions were studied to define a reproducible and robust process. By adjusting the ink properties, this method can be applied in different printing and coating techniques. Here we report on two techniques, namely spin-coating and inkjet printing. Active area efficiencies of 12.8% and 12.2% have been achieved for In_2S_3-buffered solar cells respectively, matching the performance of CdS-buffered cells prepared with the same batch of absorbers.

1 Introduction

While the industrial production of chalcopyrite solar modules relies on vacuum-based deposition for most of the layers, there are in addition efforts to implement alternative vacuum-free methods. Among them, printing technologies are deemed attractive because of superior utilization of raw materials and the potential for high throughput roll-to-roll fabrication. Developments in this area have been concentrating mainly on the chalcopyrite absorber [1,2]. The buffer layer, either CdS or, preferably, a Cd-free material such as Zn(O,S) [3,4] or In_2S_3 [5–10], can be prepared by dry as well as solution-based processes. The latter are typically implemented by chemical bath deposition and could be combined with a printed absorber to implement vacuum-free manufacturing of the core components of the cell. Nevertheless, printing the buffer layer could offer additional advantages in terms of material usage, in-line integration and with respect to the amount of (liquid) waste generated. In addition, certain printing technologies (such as inkjet printing [11]) provide highly localized deposition, direct patterning (without lithography) of materials in atmospheric environment and excellent raw material utilization. This is very attractive for the implementation of advanced cell concepts such as micro-concentrator cells [12].

In this work, precursor inks (molecular inks) were developed and combined with drying and annealing steps for the fabrication of In_2S_3 buffers. By tuning the rheological properties of the inks, both, spin-coating as well as inkjet printing could be implemented. By optimizing the composition of the precursor ink as well as the processing conditions, cells with more than 12% active area efficiency were achieved for both process variants.

2 Experimental

The precursor-based processing of indium sulphide thin films consists of four steps (see Fig. 1): (i) formulation of metal salt precursor inks, (ii) spin coating/inkjet printing, (iii) pre-heating of deposited inks and (iv) annealing in H_2S/Ar atmosphere. Firstly, a precursor ink was formulated by adding 1 mmol $In(NO_3)_3$ (Sigma-Aldrich, 99.99%) and 1.5 mmol thiourea ($SC(NH_2)_2$, Merck, 99%) to an ethanol-based solvent (containing 9 mL ethanol and 1 mL ethylene glycol). Assuming that each thiourea molecule results in one free sulphur atom, the In/S ratio was then in nominal accordance with the stoichiometry of the In_2S_3 compound. However, different ratios were used in the experiments to study the influence on the cell performance. The ink was subjected to continuous stirring until it became transparent. Secondly, the precursor ink was deposited by either spin coating or inkjet printing onto substrates. For inkjet printing, a PiXDRO LP50 inkjet printer (Roth & Rau B.V.) and an industrial-grade Trident 256Jet^{TM} printhead (Trident, ITW) were used. The Trident print head has 256 piezoelectric nozzles, each with a diameter of 50 μm and a nominal drop volume

[a] e-mail: lan.wang@helmholtz-berlin.de

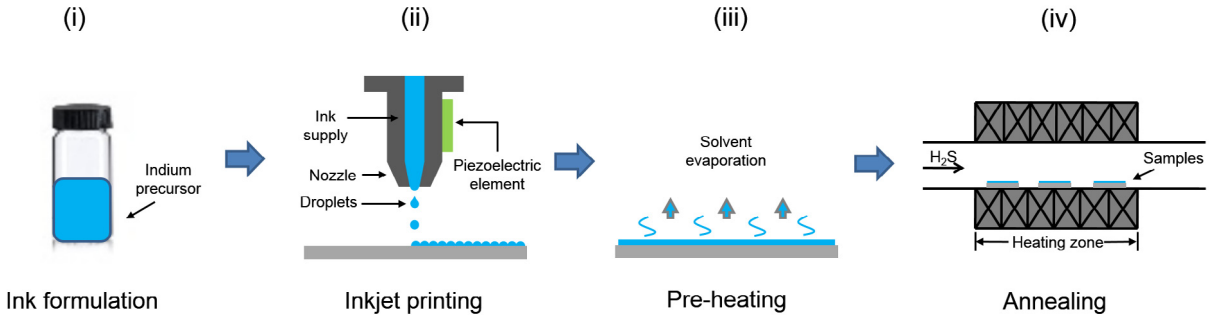

Fig. 1. Schematic diagram of In_2S_3 thin film formation process.

of 15−20 pL. The applied voltage and pulse duration of each nozzle can be tuned to obtain a well-jetted string of droplets. By increasing the resolution (dots per inch, dpi) of the printed pattern, deposited droplets can merge into a continuous film. The resolution used in our experiment was 500 dpi, in both X and Y directions. Then the sample was pre-heated in air at 150 °C for 1 min to evaporate the solvents and dry the film. Finally the pre-heated dry film was annealed in a quartz-tube furnace at 225 °C for 10 min under 5% H_2S in Ar atmosphere to drive the formation of an In_2S_3 thin film. The quartz tube was evacuated and filled with argon three times before starting annealing.

The structure of In_2S_3 thin films deposited onto glass substrates was characterized by X-ray diffraction (XRD) operated in a 2θ range of 10−70° on a Bruker D8-Advance X-ray diffractometer with Cu $K\alpha 1$ radiation at an incident angle of 0.5° (grazing incidence mode), using a step size of 0.02° and step time of 5 s. The thickness and morphology of buffer layers were analyzed in a LEO 1530 GEMINI scanning electron microscope (SEM) of Zeiss. The SEM images were recorded at an acceleration voltage of 10 kV.

Test solar cells were fabricated by depositing the In_2S_3 buffers onto soda lime glass/Mo/absorber thin film stacks (cut down to a sample size of 2.5 × 2.5 cm^2) from our in-house large-area baseline. The sequential processing of $Cu(In,Ga)Se_2$ absorbers relies on the chalcogenization of a multi-layered sputtered metal CuGa/In precursor, which is performed in nitrogen at atmospheric pressure using elemental Se [13]. Reference cells with chemical bath deposited CdS buffers were made with absorbers from the same batch. All devices were completed with an i-ZnO/ZnO:Al window layer and Ni/Al grids. Mechanical scribing was applied on each sample to define 8 solar cells with an area of 0.5 cm^2. Solar cells were measured under simulated AM 1.5 illumination and standard conditions. The cells were not annealed or light-soaked before the measurements. The quantum efficiency was recorded using Xe arc and halogen lamps and a monochromator and referenced to calibrated Si and Ge solar cells. The short-circuit current densities measured with the sun simulator were slightly too high due to spectral mismatch. Unless stated otherwise, the values given below were calculated from the measured quantum efficiency (EQE) measurement using a tabulated AM 1.5 reference spectrum and refer to the active area of the devices [14].

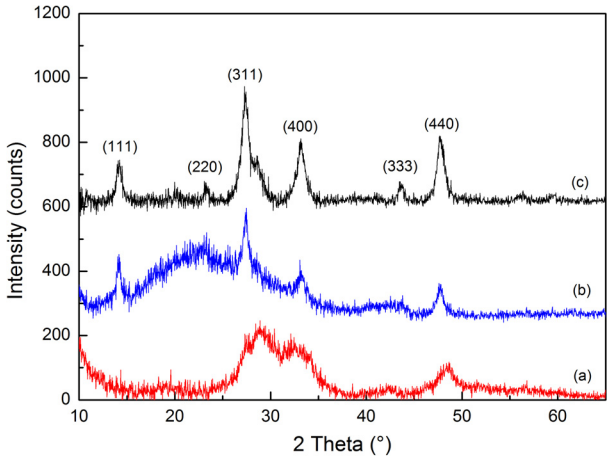

Fig. 2. XRD patterns of indium sulfide films prepared from precursor inks drop-cast onto glass substrates, (a) thiourea-containing precursor annealed in air, (b) thiourea-free precursor annealed in H_2S and (c) thiourea-containing precursor annealed in H_2S. The annealing time was 30 min for all samples.

3 Results

To confirm that the formation of In_2S_3 is possible in principle, precursor ink was drop-cast onto rinsed glass substrates followed by a pre-heating step in air at 150 °C for 1 min to remove residual solvents. XRD patterns of this pre-heated film showed no peak and further annealing in air for 30 min led to broad peaks with low intensity (see Fig. 2a). Instead, when sulfurized in Ar/H_2S at 225 °C for 30 min, the film showed pronounced XRD peaks (Fig. 2c) corresponding to β-In_2S_3(JCPDS 00-025-0390) phases, which indicates the formation of crystalline film at this moderate annealing temperature. To identify the influence of thiourea, as a sulphur source, on the formation of In_2S_3, precursor ink without thiourea was also used for structural characterization. However, the XRD pattern of the obtained film shown in Figure 2b indicates inferior crystallinity. Compared to Figure 2c, the intensities of (311) and (400) reflections were decreased and embedded in a background presumably stemming from an amorphous phase.

By adjusting the spin coating parameters, a buffer layer with a thickness of ca. 30 nm (after annealing) could

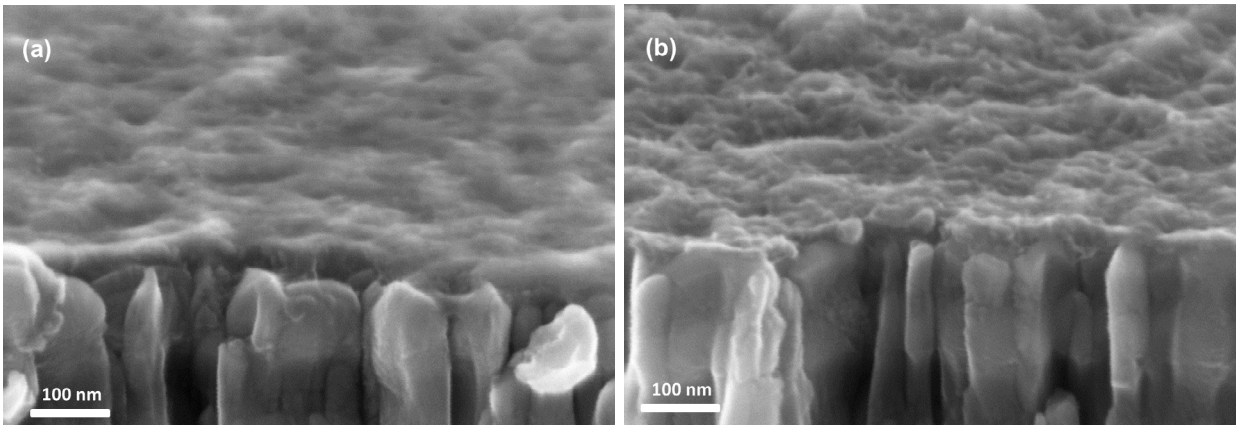

Fig. 3. SEM images of spin-coated films on glass/Mo substrates: (a) precursor film after pre-heating and (b) after annealing.

Table 1. Device parameters (best cells) of CIGSe solar cells with standard CdS buffer, spin-coated (C-03, C-04, C-05 and C-06) and inkjet-printed (C-72, C-77) In_2S_3 buffers. Sample C-03 was prepared from the thiourea-free precursor, while C-04, C-05 and C-06 were spin-coated from precursors with varied In-S ratio 1:1, 1:2 and 1:3 respectively. C-72 was prepared with the buffer annealed only in argon atmosphere (without H_2S), while C-77 was annealed in H_2S-containing atmosphere.

Sample	In/S ratio	*Voc* (mV)	*Jsc* (mA/cm^2)	*FF* (%)	η (%)
CdS	–	511	39.1	63	12.5
C-03	–	389	39.6	49	7.6
C-04	1:1	478	39.9	55	10.4
C-05	1:2	491	39.2	66	12.8
C-06	1:3	485	38.6	61	11.5
C-72	1:2	458	37.5	63	10.8
C-77	1:2	481	38.6	65	12.2

be achieved. The cross-sections of spin-coated films on a glass/Mo substrate before and after annealing are shown in Figure 3. The thickness of the film after annealing was slightly reduced (from 34 nm to 28 nm in the given SEM images). Inkjet-printed films were similar in morphology on a microscopic level but slightly thinner (25 nm before and 20 nm after annealing, respectively). In terms of material utilization, this drop-on-demand technique is superior to spin coating. For instance, only 4 μL ink is needed to inkjet print a buffer layer on a standardized sample, in comparison with 100 μL ink required for spin coating.

Photovoltaic parameters of solar cells from a typical test run (best cells) are summarized in Table 1. To achieve the optimal solar cell efficiency, variations of the In/S ratio (1:1, 1:2 and 1:3) in the precursor were applied. The highest efficiency (12.8%) was obtained with the In/S ratio of 1:2 (C-05). The sample fabricated from the thiourea-free precursor (C-03) showed lower open-circuit voltage and fill factor compared to samples produced with thiourea-containing precursors. The transfer of the processing route from spin-coating to inkjet printing was successfully implemented, with the best cell efficiency of 12.2% (C-77).

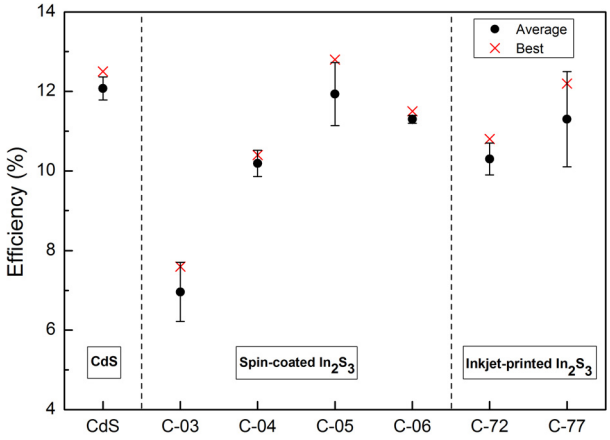

Fig. 4. Average (16 cells) and best efficiencies of solar cells buffered with CdS, spin-coated In_2S_3 and inkjet-printed In_2S_3. The error bars represent the standard deviation.

Solar cells with a buffer annealed in pure argon (C-72) showed only slightly lower efficiency. For each experimental condition, two 2.5 × 2.5 cm^2 samples have been prepared identically, each containing 8 cells. The average and best efficiencies of the cells are depicted in Figure 4. The trend of the average of cell efficiencies upon different processing conditions corresponds well with the best values and all the data are within a reasonable deviation range.

The current-voltage (J-V) characteristics and external quantum efficiencies (EQE) of selected best cells from Table 1 are presented in Figure 5. The J-V curves of both cells with solution-processed In_2S_3 demonstrate diode properties (shunt and series resistance, diode quality factor) leading to fill factors that are even slightly higher than that of the CdS reference. The EQE measurements show a good photocurrent collection with a maximum of about 90% at a wavelength between 650 nm and 680 nm.

4 Discussion

The best results were achieved by annealing in a sulphur containing atmosphere but reasonable performance

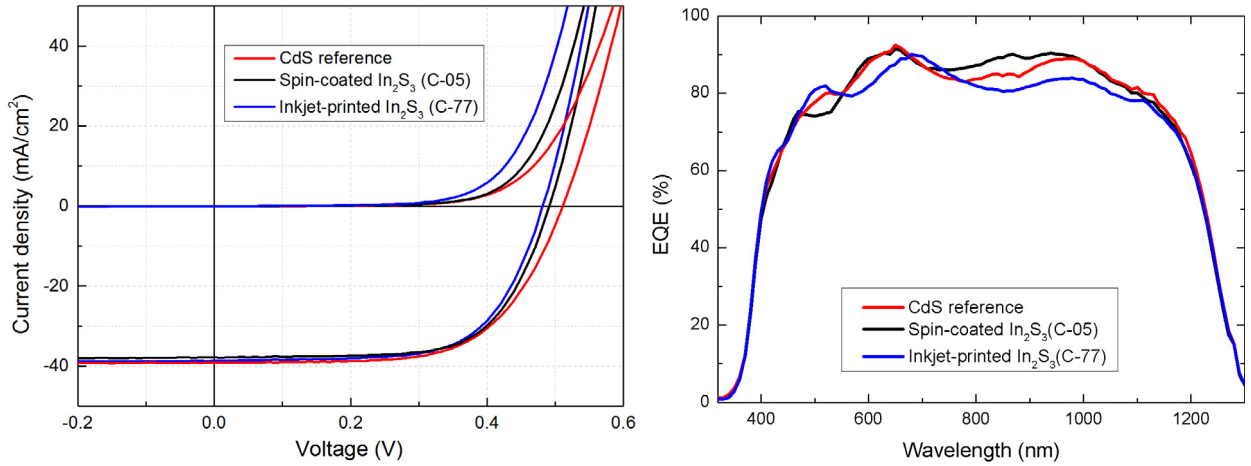

Fig. 5. Comparison of dark and illuminated current-voltage (J-V) characteristics (left, current densities as measured, without correction for spectral mismatch) and external quantum efficiencies (right) of three best solar cells buffered with standard CdS, spin-coated In_2S_3 and inkjet-printed In_2S_3, respectively.

was also achieved using an inert, sulphur-free atmosphere (sample C-72 in Tab. 1). In contrast, adding a source of sulphur (preferably with S/In = 2) to the ink appears to be crucial, as judged from the XRD patterns as well as cell data. The influence of thiourea on crystallization, phases, and final structure of the In_2S_3 buffer needs to be investigated in more detail, also taking into account the possible out diffusion of sodium and copper from the absorber. A universally applicable ink should be non-corrosive (pH) and stable, i.e. should not produce precipitations even with prolonged storage. Besides the potential formation of $In_x(OH)$, the required sulphur content may lead to $In_x(OH,S)_y$ precipitation. Certain solutions can indeed be used to grow layers (chemical bath deposition of $In_x(OH,S)_y$ [15]. It is therefore not surprising that initial efforts to formulate stable and non-corrosive water-based inks were not successful. Different metal salts and organic solvents have then been tested and lead to the simple approach used here, i.e. $In(NO_3)_3$ and thiourea in ethanol. Addition of ethylene glycol allows tuning the viscosity of the ink according to the requirements of the deposition method. This solvent system was observed to be stable under ambient temperature over months. A single coating step is sufficient to achieve a thickness suitable for buffer layers. This is different from the deposition of absorbers which requires multi-coatings with intermediate preheating steps in order to reach a micrometer-scale thickness [11]. Therefore the as-deposited buffer layer can be annealed directly without the pre-heating/drying step (confirmed in experiments not shown here). Besides annealing in inert (pure argon) atmosphere, this is another possible simplification of the process that could lower production costs. In this context, note that the annealing step used here to synthesize the compound appears to eliminate the need for post-deposition annealing of the completed device typically required for evaporated In_2S_3 buffers [16]. Higher annealing temperatures than those used in our work are assumed to further increase the crystallinity of the films. However, it is known from In_2S_3 buffers prepared by other technologies that the junction properties are degrading when the annealing temperature is too high [17] or the annealing time too long, due to Cu, Ga and In interdiffusion between the absorber and the buffer. A possible disadvantage of the process is contamination (C, O, N) stemming from the organic solvents, drying in air, decomposition of thiourea, or the In-salt. Also the use of toxic H_2S, if not avoidable, may counterbalance the reduced amount of liquid waste.

Our In_2S_3 buffer, even in preliminary experiments, showed almost identical results to the CdS buffer in terms of homogeneity and cell parameters, suggesting that this route is stable with a wide process window. The potential with respect to different types of absorbers (including those capable of higher efficiency) needs to be verified in further work. Judging from the red response the current transport properties of the absorber are not adversely affected by the buffer layer preparation. Based on the experience with other deposition methods, the blue response with a thin In_2S_3 buffer is often slightly higher than that of CdS-buffered devices [10,18]. This is not clearly observed here, partly because the blue response of the reference cell is already quite high (thin CdS). The blue response is influenced not only by the buffer layer transparency, but also by interference fringes and the collection probability of charge carriers generated close to the interface. The latter can be reduced when the there is an extended inversion zone (low absorber doping) [19]. A comparison of the optical absorption of films deposited on glass and the quantum efficiency of the cells suggests that this may play a role here but more experiments are needed to judge the blue response achievable with our printed buffers.

5 Summary

A precursor ink based process for preparing In_2S_3 buffer layers was proposed. By tuning the solution compositions, stable inks with suitable rheological properties

were formulated. In_2S_3 thin films could be obtained by annealing the precursor films in a H_2S-containing atmosphere at 225 °C as verified by XRD. The addition of thiourea to the precursor ink was found to improve the crystallinity of the films as well as cell performance. Successful implementation of ink deposition by spin coating or inkjet printing on CIGSe absorbers led to working solar cells with 12.8% and 12.2% efficiency respectively, which is comparable to CdS-buffered solar cells prepared from the same batch of absorbers.

The research leading to these results has received funding from the European Union Seventh Framework Programme (FP7/2007-2013) under grant agreement no. 609788 (CHEETAH project). The authors thank C. Kelch, M. Kirsch, M. Hartig for completion of the devices.

References

1. S.M. McLeod, C.J. Hages, N.J. Carter, R. Agrawal, Prog. Photovolt.: Res. Appl. **23**, 1550 (2015)
2. T.K. Todorov, O. Gunawan, T. Gokmen, D.B. Mitzi, Prog. Photovolt.: Res. Appl. **21**, 82 (2013)
3. R. Klenk, A. Steigert, T. Rissom, D. Greiner, C.A. Kaufmann, T. Unold, M.C. Lux-Steiner, Prog. Photovolt: Res. Appl. **22**, 161 (2014)
4. T.M. Friedlmeier, P. Jackson, A. Bauer, D. Hariskos, O. Kiowski, R. Wuerz, M. Powalla, IEEE J. Photovolt. **5**, 1487 (2015)
5. C. Hönes, J. Hackenberg, S. Zweigart, A. Wachau, F. Hergert, S. Siebentritt, J. Appl. Phys. **117**, 094503 (2015)
6. R. Sáez-Araoz, J. Krammer, S. Harndt, T. Koehler, M. Krueger, P. Pistor, A. Jasenek, F. Hergert, M.C. Lux-Steiner, C.-H. Fischer, Prog. Photovolt: Res. Appl. **20**, 855 (2012)
7. T. Todorov, J. Carda, P. Escribano, A. Grimm, J. Klaer, R. Klenk, Sol. Energy Mater. Sol. Cells **92**, 1274 (2008)
8. M. Bär, N. Allsop, I. Lauermann, C.H. Fischer, Appl. Phys. Lett. **90**, 132118 (2007)
9. B. Yahmadi, N. Kamoun, R. Bennaceur, M. Mnari, M. Dachraoui, K. Abdelkrim, Thin Solid Films **473**, 201 (2005)
10. N.A. Allsop, A. Schönmann, H.J. Muffler, M. Bär, M.C. Lux-Steiner, C.H. Fischer, Prog. Photovolt: Res. Appl. **13**, 607 (2005)
11. X. Lin, J. Kavalakkatt, M.C. Lux-Steiner, A. Ennaoui, Adv. Sci. **2**, 1500028 (2015)
12. M. Paire, L. Lombez, J.-F.O. Guillemoles, D. Lincot, J. Appl. Phys. **108**, 034907 (2010)
13. B. Rau, F. Friedrich, N. Papathanasiou, C. Schultz, B. Stannowski, B. Szyszka, R. Schlatmann, Photovolt. Int. **17**, 99 (2012)
14. ASTM G173-03 (2012), *Standard Tables for Reference Solar Spectral Irradiances: Direct Normal and Hemispherical on 37° Tilted Surface*, (W.C. ASTM International, PA, 2012), www.astm.org
15. D. Hariskos, M. Ruckh, U. Rühle, T. Walter, H.W. Schock, J. Hedström, L. Stolt, Sol. Energy Mater. Sol. Cells **41-42**, 345 (1996)
16. P. Pistor, N. Allsop, W. Braun, R. Caballero, C. Camus, C.H. Fischer, M. Gorgoi, A. Grimm, B. Johnson, T. Kropp, I. Lauermann, S. Lehmann, H. Mönig, S. Schorr, A. Weber, R. Klenk, Phys. Stat. Sol. A **206**, 1059 (2009)
17. D. Abou-Ras, G. Kostorz, D. Hariskos, R. Menner, M. Powalla, S. Schorr, A.N. Tiwari, Thin Solid Films **517**, 2792 (2009)
18. P. Pistor, A. Grimm, D. Kieven, F. Hergert, A. Jasenek, R. Klenk, in: *Proceedings 37th IEEE Photovoltaic Specialists Conference (PVSC), Seattle, 2011*, p. 002808
19. R. Klenk, H.W. Schock, in: *Proceedings 12th European Photovoltaic Solar Energy Conference (EU PVSEC), Amsterdam, 1994*, p. 1588

Cite this article as: Lan Wang, Xianzhong Lin, Ahmed Ennaoui, Christian Wolf, Martha Ch. Lux-Steiner, Reiner Klenk, Solution-processed In_2S_3 buffer layer for chalcopyrite thin film solar cells, EPJ Photovoltaics **7**, 70303 (2016).